Journal of Neurochemistry

JOURNAL OF NEUROCHEMISTRY | 2013 | 126 | 579–590 doi: 10.1111/jnc.12333

ORIGINAL ARTICLE

Glutamatergic and GABAergic energy metabolism measured in the rat brain by ^{13}C NMR spectroscopy at 14.1 T

João M. N. Duarte*,† and Rolf Gruetter*,†,‡

*Laboratory for Functional and Metabolic Imaging, École Polytechnique Fédérale de Lausanne, Lausanne, Switzerland

†Department of Radiology, University of Lausanne, Lausanne, Switzerland

‡Department of Radiology, University of Geneva, Geneva, Switzerland

Abstract

Energy metabolism supports both inhibitory and excitatory neurotransmission processes. This study investigated the specific contribution of astrocytic metabolism to γ-aminobutyric acid (GABA) synthesis and inhibitory GABAergic neurotransmission that remained to be ilucidated *in vivo*. Therefore, we measured ^{13}C incorporation into brain metabolites by dynamic ^{13}C nuclear magnetic resonance spectroscopy at 14.1 T in rats under α-chloralose anaesthesia during infusion of [1,6-^{13}C]glucose. The enhanced sensitivity at 14.1 T allowed to quantify incorporation of ^{13}C into the three aliphatic carbons of GABA non-invasively. Metabolic fluxes were determined with a mathematical model of brain metabolism comprising glial, glutamatergic and GABAergic compartments. GABA synthesis rate was 0.11 ± 0.01 μmol/g/min. GABA-glutamine cycle was 0.053 ± 0.003 μmol/g/min and accounted for 22 ± 1% of total neurotransmitter cycling between neurons and glia. Cerebral glucose oxidation was 0.47 ± 0.02 μmol/g/min, of which 35 ± 1% and 7 ± 1% was diverted to the glutamatergic and GABAergic tricarboxylic acid cycles, respectively. The remaining fraction of glucose oxidation was in glia, where 12 ± 1% of the TCA cycle flux was dedicated to oxidation of GABA. 16 ± 2% of glutamine synthesis was provided to GABAergic neurons. We conclude that substantial metabolic activity occurs in GABAergic neurons and that glial metabolism supports both glutamatergic and GABAergic neurons in the living rat brain.

Keywords: ^{13}C NMR, brain, GABA, glucose, glutamate, metabolism.

J. Neurochem. (2013) **126**, 579–590.

The vast majority of synapses in the central nervous system use either glutamate or γ-aminobutyric acid (GABA) to mediate excitatory or inhibitory neurotransmission. Although glutamatergic synapses outnumber GABAergic synapses and the energetic requirements of excitatory neurons are considered higher than those of inhibitory neurons, a substantial amount of glucose, the main substrate for cerebral energy metabolism, has been suggested to be oxidized in inhibitory GABAergic neurons (e.g. Patel *et al.* 2005; Calvetti and Somersalo 2012; Howarth *et al.* 2012).

Nuclear magnetic resonance (NMR) spectroscopy has been used to probe metabolic pathways *in vivo* upon infusion of specific ^{13}C-enriched substrates (Gruetter 2002). However, GABA metabolism *in vivo* remains difficult to study because of its low concentration. Although several attempts were made to detect ^{13}C turnover curves of GABA, the dynamic measurement of GABA enrichment was restricted to only one or two carbons (Pfeuffer *et al.* 1999; Yang *et al.* 2005; van Eijsden *et al.* 2010). Therefore, studies of brain metabolism mostly focused on glutamatergic function, as glutamate is present in much higher concentrations. Determination of the activity of GABAergic metabolic pathways is important since GABA metabolism has been implicated in neurological

Received January 24, 2013; revised manuscript received June 5, 2013; accepted June 6, 2013.

Address correspondence and reprint requests to João M. N. Duarte, EPFL SB IPMC LIFMET, Station 6 (Bâtiment CH), CH-1015 Lausanne, Switzerland. E-mail: joao.duarte@epfl.ch

Abbreviations used: CMR_{glc}, cerebral metabolic rate for glucose consumption; CRLB, Cramér-Rao lower bound; DEPT, distortionless enhancement by polarization transfer; FE, fractional enrichment; GABA-T, GABA-transaminase; GABA, γ-aminobutyric acid; GAD, glutamate decarboxylase; NMR, nuclear magnetic resonance; PCA, perchloric acid; SSADH, succinic-semialdehyde dehydrogenase; SSA, succinic-semialdehyde; TCA cycle, tricarboxylic acid cycle.

disorders (reviewed in Choi and Shen 2012; Waagepetersen *et al.* 1999): several psychiatric disorders were found to be associated with modification of inhibitory GABAergic function, GABA metabolism and/or GABA levels; in epilepsy, inhibition of GABA-transaminase (GABA-T, EC 2.6.1.19) or GABA transporters increases synaptic GABA availability, which correlates with reduced glucose consumption and improved seizure control.

GABA metabolism occurs in the GABA shunt (e.g. Choi and Shen 2012). Briefly, GABA is synthesized in the cytosol from glutamate by glutamate decarboxylase (GAD, EC 4.1.1.15) and is catabolized in mitochondria, starting with GABA conversion to succinic-semialdehyde (SSA) in mitochondria by GABA-T, with simultaneous amination of 2-oxoglutarate to glutamate, and then SSA catabolism to succinate by SSA dehydrogenase (SSADH, EC 1.2.1.24), for dual use in the tricarboxylic acid (TCA) cycle, and as electron donor of the mitochondrial electron transport chain. After synaptic release, GABA is believed to be mostly cleared by neurons as GABA transporters are less abundant in glial than neuronal membranes (Conti *et al.* 2004). Nevertheless, uptake of GABA by astrocytes and further metabolism through the GABA shunt, as well as glutamine provision to GABAergic neurons by the GABA-glutamine cycle, have been reported (Schousboe and Waagepetersen 2003, 2007; Bak *et al.* 2006). In previous ^{13}C NMR spectroscopy studies designed to quantify metabolic fluxes of GABA metabolism in the brain *in vivo*, astrocytic fluxes were either constrained to those in neurons or determined in parallel experiments using ^{13}C-enriched acetate that is principally oxidized in glia (e.g. Patel *et al.* 2005; van Eijsden *et al.* 2010). Therefore, the effective contribution of astrocytic metabolism to GABAergic neurotransmission remains to be addressed *in vivo*. The aim of this study was to determine compartmentalized metabolic fluxes in GABAergic neurons and connecting astrocytes using the resonances of all three aliphatic carbons of GABA at 14.1 T in the living rat brain.

Materials and methods

Animals

All experimental procedures involving animals were approved by the local ethics committee (EXPANIM-SCAV, Switzerland). Male Sprague–Dawley rats (267 ± 25 g, $n = 8$, purchased to Charles River Laboratoires, L'Arbresle, France) were prepared as previously detailed in Duarte *et al.* (2009). Briefly, animals were mechanically ventilated with a mixture of 30% O_2 in air using pressure-driven ventilator (MRI-1, CWE incorporated, Ardmore, PA, USA), and catheters were placed into a femoral artery for collection of blood samples and into a femoral vein for infusion of saline solutions containing α-chloralose (Acros Organics, Geel, Belgium) or [1,6-^{13}C]glucose (Sigma-Aldrich, Basel, Switzerland). Light anaesthesia was achieved by administration of α-chloralose (bolus of 80 mg/kg and continuous infusion of 28 mg/kg/h). Arterial blood pressure, heart rate and respiratory rate were continuously monitored with an animal monitoring system (SA Instruments, Stony Brook, NY, USA). Blood samples were collected every 20–30 min to measure gases, pH, lactate and glucose. Arterial pH and pressures of O_2 and CO_2 were measured using a blood gas analyser (AVL Compact 3; Diamond Diagnostics, Holliston, MA, USA) and were maintained within the normal physiological range by adjusting respiratory rate and volume. Body temperature was maintained between 37.0 and 37.5°C. Plasma glucose and lactate concentrations were quantified with the glucose and lactate oxidase methods, respectively, using two multi-assay analysers (GW7 Micro-Stat; Analox Instruments, London, UK). The [1,6-^{13}C]glucose infusion procedure was previously described in Duarte *et al.* (2011) and allowed to achieve a sustained plasma fractional enrichment (FE) of 70%, which was confirmed by NMR spectroscopy of collected plasma samples.

NMR spectroscopy

All *in vivo* NMR experiments were carried out in a DirectDrive spectrometer (Agilent Technologies, Palo Alto, CA, USA) interfaced to a 26-cm horizontal bore 14.1 T magnet (Magnex Scientific, Abingdon, UK), using a homebuilt coil consisting of a ^{1}H quadrature surface coil and a ^{13}C linearly polarized surface coil (Duarte *et al.* 2011). Animals were immobilized in a home-built holder with a bite bar and two ear inserts to minimize potential motion. The rat brain was positioned in the isocenter of the magnet and fast-spin-echo images with repetition time of 4 s, echo time of 52 ms and echo train length of 8 allowed to identify anatomical landmarks, which were used to place the volume of interest (VOI) of 320 μL in the brain. After FAST(EST)MAP shimming (Gruetter 1993; Gruetter and Tkác 2000), localized ^{1}H NMR spectra were acquired using STEAM with echo time of 2.8 ms, mixing time of 20 ms and repetition time of 4 s (Tkác *et al.* 2003; Mlynárik *et al.* 2006). ^{13}C NMR spectra were acquired using semi-adiabatic distortionless enhancement by polarization transfer (DEPT) combined with 3D-ISIS ^{1}H localization (Henry *et al.* 2003a).

Analysis of ^{1}H and ^{13}C NMR spectra was carried out using LCModel (Stephen Provencher Inc., Oakville, ON, Canada) as described by Mlynárik *et al.* (2006) and Henry *et al.* (2003b), respectively. The scaling of dynamically measured ^{13}C concentrations was based on the FE determined *in vitro* in ^{13}C NMR spectra from perchloric acid extracts of the brain prepared at the end of each experiment (detailed in Duarte *et al.* 2011). High-resolution *in vitro* NMR spectroscopy was performed as described in Duarte *et al.* (2007) using a 14.1 T DRX-600 spectrometer equipped with a 5 mm cryoprobe (Bruker BioSpin SA, Fallenden, Switzerland).

In general, total concentration of brain metabolites was determined by ^{1}H NMR spectroscopy. Since glutamine levels from ^{1}H NMR spectra *in vivo* were lower than ^{13}C-enriched glutamine in ^{13}C NMR spectra, total glutamine was calculated with the relation between FE and the ^{13}C content at steady state. FE is defined as $FE = \frac{[^{13}C]}{[^{12}C]+[^{13}C]}$, which can be written as follows: $FE\frac{[^{12}C]+[^{13}C]}{[^{13}C]} = 1$, where $[^{13}C]$ and $[^{12}C] + [^{13}C]$ represent the concentration of ^{13}C label and the total concentration in a given carbon, respectively. For glutamate and glutamine C3, one can consider that

$$\frac{FE_{Gln\,C3}}{[Gln\,C3]}[Gln] = \frac{FE_{Glu\,C3}}{[Glu\,C3]}[Glu]$$

Assuming that the probability of ^{13}C enrichment in C3 through metabolism in the TCA cycle(s) is the same for molecules with or without labelling in C4, FE_{C3} = C4D34/(C4S + C4D34) for both glutamate (Glu) and glutamine (Gln), where C4D34 and C4S are, respectively, the doublet and singlet in the resonance of C4 from either glutamine or glutamate (e.g. Malloy *et al.* 1987; Gruetter *et al.* 1994; Mason *et al.* 1995). Because C5 does not become labelled upon infusion of [1,6-^{13}C]glucose, the total C4 signal corresponds to C4S + C4D34. Thus, the equation above can be rewritten using ^{13}C measured signals at steady state:

$$[Gln] = \frac{Gln\,C3}{\frac{Gln\,C4D34}{Gln\,C4}} \times \frac{\frac{Glu\,C4D34}{Glu\,C4}}{Glu\,C3}[Glu]$$

Determination of metabolic fluxes and statistical analysis

Kinetic modelling of [1,6-^{13}C]glucose metabolism in glutamatergic, GABAergic and glial compartments was performed by extension of the mathematical model of compartmentalized cerebral metabolism previously described (Duarte *et al.* 2011). Figure 1 depicts the metabolic pools and fluxes defined in the three-compartment model, which is detailed in Appendix. Variations to this model were tested and are subject of discussion (see below). In particular, the inclusion of a glutamine pool exchangeable through V_{ex}^{g} leads to a major fit improvement. Mathematical models were adjusted to the eleven ^{13}C enrichment curves of glutamate, glutamine and GABA C2, C3 and C4, and of aspartate C2 and C3, using the Levenberg–Marquardt algorithm for non-linear regression, coupled to a Runge-Kutta method for non-stiff systems to obtain numerical solutions of the ordinary differential equations that define the model (detailed in the Appendix). Significance of the fitted parameters (fluxes) was inferred from *t*-statistics. *F*-statistics was used for relative assessment of fit quality. Because accuracy in flux estimation is inversely proportional to the noise level of experimental data (Shestov *et al.* 2007), ^{13}C enrichment curves were averaged from all rats rather than fitting individual time courses. Then, reliability of determined fluxes was evaluated by Monte-Carlo analysis, in which Gaussian noise with the same variance of fit residuals was added to the best fit and initial conditions were randomly generated within confidence interval of the obtained value. Typically, 500 simulated data sets were created for each individual analysis. The estimated metabolic fluxes are shown as mean ± SD, being the SD resulting from fitting a Gamma function to the probability distribution obtained with the Monte-Carlo

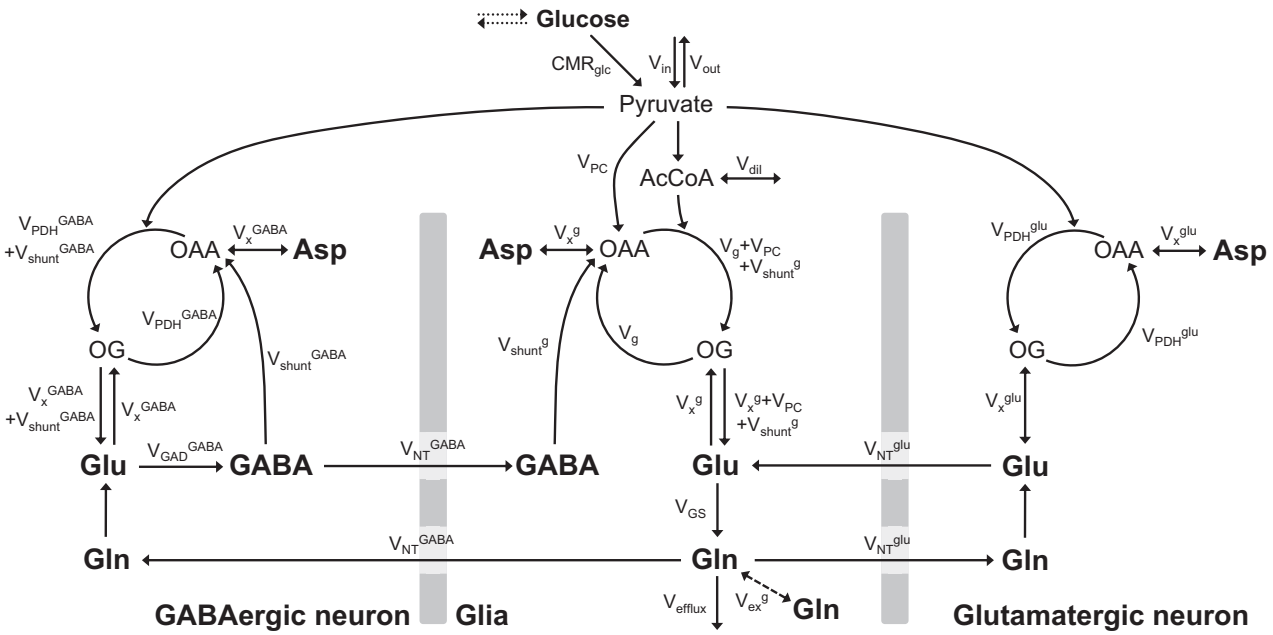

Fig. 1 Three-compartment model of brain metabolism. CMR_{glc} is the total cerebral metabolic rate of glucose. Pyruvate originated from glucose consumption is in fast equilibrium with lactate that is exchanged between neurons and glia and is diluted with extra-cerebral lactate through V_{out}/V_{in}. V_{PDH}^{glu} accounts for the total TCA cycle flux in glutamatergic neurons, $V_{PDH}^{GABA} + V_{shunt}^{GABA}$ is the total GABAergic TCA cycle, $V_g + V_{PC} + V_{shunt}^{g}$ is the total glial TCA cycle, V_{PC} is the rate through pyruvate carboxylase. In the glial compartment, the dilution of label at the level of acetyl-CoA (AcCoA) by glial-specific substrates is accounted by V_{dil}. TCA cycle intermediates oxaloacetate (OAA) and 2-oxoglutarate (OG) exchange with amino acids through the exchange flux V_X. The glutamate-glutamine and GABA-glutamine cycles are V_{NT}^{glu} and V_{NT}^{GABA}, respectively, and glutamine synthetase rate is V_{GS}. The GABA synthesis rate catalysed by glutamate decarboxylase (V_{GAD}) was restricted to GABAergic neurons. V_{shunt}^{g} and V_{shunt}^{GABA} represent the oxidation of GABA in the glial and GABAergic compartments, respectively. Finally, efflux of labelling from the metabolic system occurs through the rate of glial glutamine loss V_{efflux}. An additional glutamine pool in exchange via V_{ex}^{g} was tested as described in the text. The superscripts g, glu and GABA distinguish metabolic pools or fluxes in the glial, glutamatergic and GABAergic compartments, respectively.

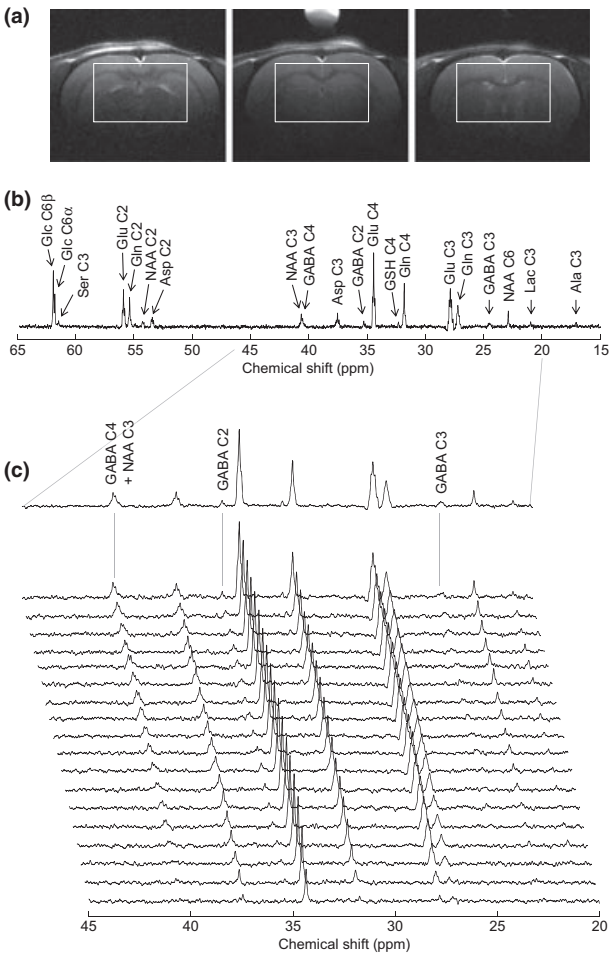

Fig. 2 ^{13}C NMR spectra acquired *in vivo* at 14.1 T from the rat brain upon infusion of [1,6-^{13}C]glucose. In (a) is represented the volume of interest (VOI) of 5 × 8×8 mm^3 in the rat brain. Brain images are 0.8 mm of thickness and spaced by 1.6 mm. The sphere in the top is the [^{13}C]formic acid reference used for calibration of radiofrequency pulses. (b) Shows a representative spectrum acquired for 1 h starting after 5 h of [1,6-^{13}C]glucose infusion, with identification of visible resonances (expansion from 15 to 65 ppm; Gaussian apodization with gf = 0.08, gfs = 0.02). (c) Shows the time course of spectra with 20-min time resolution acquired during 6 h starting at the onset of [1,6-^{13}C] glucose infusion. The top spectrum is the sum of the three last scans, that is, acquired for 1 h (Lorentzian-Gaussian apodization was employed with lb = 5, gf = 0.08, gfs = 0.02). Resonance assignment: Ala, alanine; Lac, lactate; NAA, *N*-acetylaspartate; GABA, γ-amino-butirate; Gln, glutamine; Glu, glutamate, GSH, glutathione; Asp, aspartate; Ser, serine; Glc, glucose.

simulations. All numerical procedures were performed using Matlab (The MathWorks, Natick, MA, USA). Data are presented as mean ± SD of eight experiments, unless otherwise stated.

Results

Upon infusion of [1,6-^{13}C]glucose, the FE of plasma glucose was 0.71 ± 0.02 after 5 min and over the whole period of ^{13}C NMR spectra acquisition. When measuring the incorporation of ^{13}C from [1,6-^{13}C]glucose into amino acids in the living rat brain using ^{13}C NMR spectroscopy at 14.1 T (volume of interest is shown in Fig. 2a), 20 carbon resonances from 10 metabolites were detected between 15 and 65 ppm (Fig. 2b), including three GABA peaks that were clearly detectable with 20 min of temporal resolution (Fig. 2c). The analysis of ^{13}C NMR spectra with LCModel allowed to simultaneously quantify not only the three GABA resonances but also their isotopomers (Fig. 3). The multiplets in carbons of GABA arising from the presence of adjacent ^{13}C resonances were observed in the ^{13}C NMR spectra *in vivo* (Fig. 3a) as well as *in vitro* in brain PCA extracts (Fig. 3b). Cramér-Rao lower bounds (CRLB) for GABA C2, C4 and C3 were below 30% from 54, 72 and 126 min after the beginning of [1,6-^{13}C]glucose infusion, respectively (Fig. 3c).

^{1}H NMR spectroscopy was used to determine the total concentration of brain metabolites that become enriched by ^{13}C (Table 1). Brain metabolite levels were found to agree with prior literature reports (Tkác *et al.* 2003; Duarte *et al.* 2011). However, total brain levels of glutamine measured by ^{1}H NMR spectroscopy *in vivo* were found to be below those of ^{13}C-enriched glutamine measured by ^{13}C NMR spectroscopy. Therefore, total glutamine was estimated at 5.3 ± 0.4 μmol/g using the relation between FE and the ^{13}C signals observed at steady-state (Table 1, discussed below).

When fitting the mathematical model to the ^{13}C time courses of glutamate, glutamine, aspartate and GABA, generally an excellent fit was observed (Fig. 4), which resulted in the metabolic fluxes in Table 2. The curves generated by the initial model were not a complete representation of the data measured *in vivo*, which is particularly clear for glutamine C4 (Fig. 4). The goodness-of-fit was improved by the inclusion of an additional exchangeable glutamine pool in the glial compartment (R^2 = 0.976 and f = 1960, vs. R^2 = 0.972 and f = 1680), as indicated by the fit residuals, that is, the mean residuals with and without this glutamine pool were −0.0034 ± 0.0244 and 0.0042 ± 0.0268 (dimension of FE) and the residual sum of squares was 0.328 versus 0.395, respectively (Fig. 4b). The exchange flux V_{ex}^{g} was found to be 0.060 ± 0.008 μmol/g/min and significantly different from zero (t = 284). The other metabolic fluxes in the model were not substantially affected by the inclusion of this additional glutamine pool (Table 2). Thus, metabolic fluxes are hereafter presented and discussed for the model that includes V_{ex}^{g}.

Total glucose oxidation, that is, cerebral metabolic rate for glucose consumption ($CMR_{glc(ox)}$), was 0.47 ± 0.02 μmol/g/min. Since glucose consumption was fixed at 0.52 μmol/g/min, as determined previously (see Appendix), net release of lactate (V_{out}) was 0.11 ± 0.03 μmol/g/min. About half of glucose oxidation was found to occur through pyruvate dehydrogenase in the glial compartment (47 ± 3%), and a considerable fraction because of pyruvate carboxylation: V_{PC}

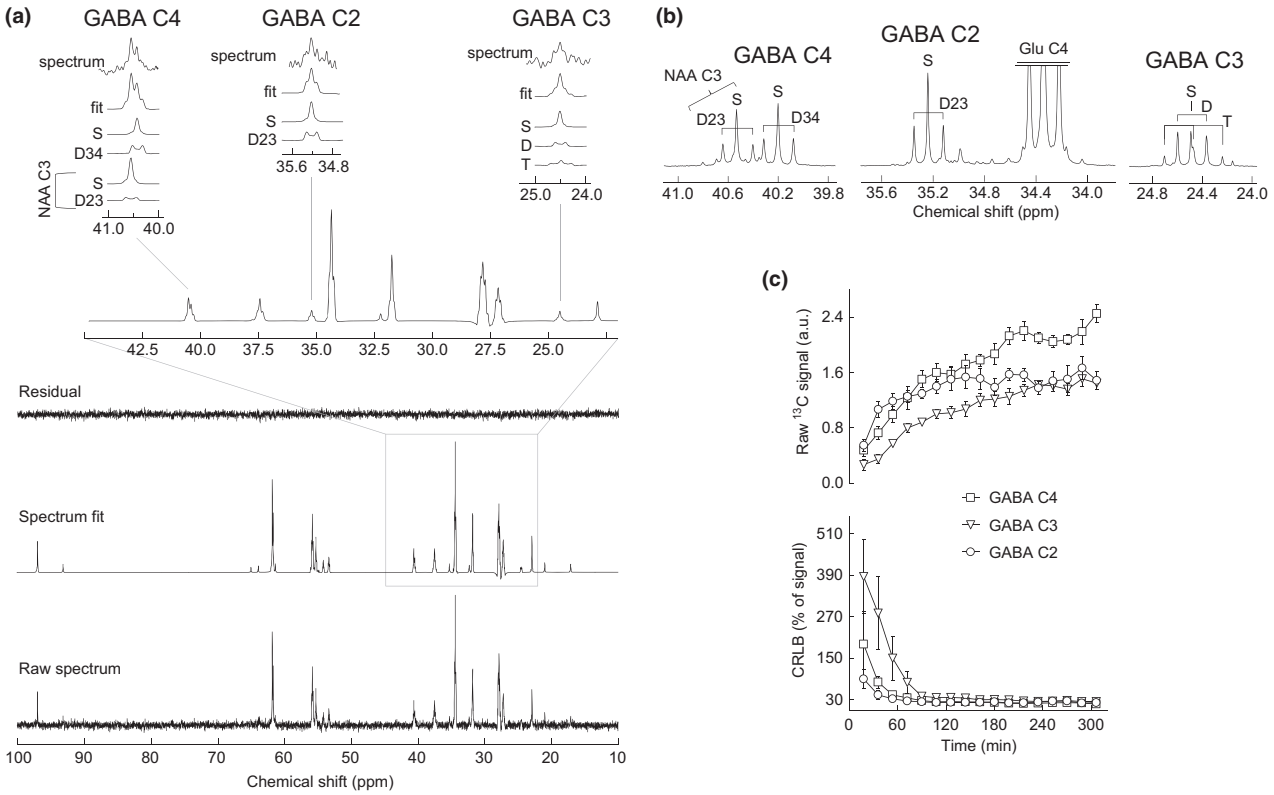

Fig. 3 (a) Depicts a typical fit obtained with LCModel for an *in vivo* ^{13}C NMR spectrum acquired for 2 h after 4 h of [1,6-^{13}C]glucose infusion. Expansions in the top of (a) show the fitting of individual isotopomers in GABA C2, C3 and C4. These were also observed in the high-resolution spectrum acquired from brain extracts after [1,6-^{13}C]glucose infusion for 6 h (b). High-resolution ^{13}C NMR spectra *in vitro* were acquired at 600 MHz, pH 7.0 and 12°C to allow separation of NAA C3 and GABA C4 resonances. (c) Shows ^{13}C signal and associated Cramér-Rao lower bound (CRLB) for GABA resonances. Signal intensity is given in arbitrary units (a.u.) and was not corrected for relative DEPT enhancement or distance from the transmit/observe frequency. Data are mean ± SEM of eight rats.

Table 1 Total cerebral concentration of metabolites observable in ^{13}C NMR spectra *in vivo* upon infusion of [1,6-^{13}C]glucose, as determined by ^{1}H NMR spectroscopy prior to substrate infusion. Concentrations are shown as mean ± SEM of eight rats

	Concentration (μmol/g)
Glutamate	8.6 ± 0.4
Glutamine	2.7 ± 0.1; [a]5.3 ± 0.4
Aspartate	2.2 ± 0.3
GABA	1.3 ± 0.1
GSH	0.91 ± 0.09
NAA	8.8 ± 0.4
Glucose	1.4 ± 0.4
Lactate	0.71 ± 0.05
Alanine	0.46 ± 0.07

[a]glutamine concentration determined through FE of glutamate and glutamine C3 in ^{13}C NMR spectra and total glutamate content.

was 10 ± 1% of $CMR_{glc(ox)}$ and 21 ± 1% of V_{TCA}^{g}. In glutamatergic and GABAergic neurons, the fraction of total glucose oxidation was 35 ± 1% and 7 ± 1%, respectively. V_{NT}^{GABA} was 22 ± 1% of total neurotransmitter cycling between neurons and astrocytes. In GABAergic neurons, V_{GAD} was 0.11 ± 0.01 μmol/g/min and V_{NT}^{GABA} was 0.053 ± 0.003 μmol/g/min, which was set to be equal to the GABAergic glutaminase flux. Thus, glial glutamine contributed to 48 ± 5% of GABA synthesis. Glial V_{TCA} and V_{GS} account for GABA recycling through the glial GABA shunt, which was 12 ± 1% of V_{TCA}^{g} and resulted in 16 ± 2% of glutamine synthesis (V_{GS}) to be shuttled to GABAergic neurons for GABA production. In total, the rate of glucose oxidation supporting GABAergic activity was 13 ± 1% ($V_{TCA}^{GABA} + V_{shunt}^{g}$). The rate of label exchange between cytosolic amino acids and their mitochondrial counterparts, namely mediated by the malate-aspartate shuttle, were on the order of the TCA cycle rate in each compartment.

Discussion

This study reports for the first time the *in vivo* measurement of the ^{13}C enrichment in all three aliphatic carbons of GABA in the rat brain, which contributed to elucidate multiple

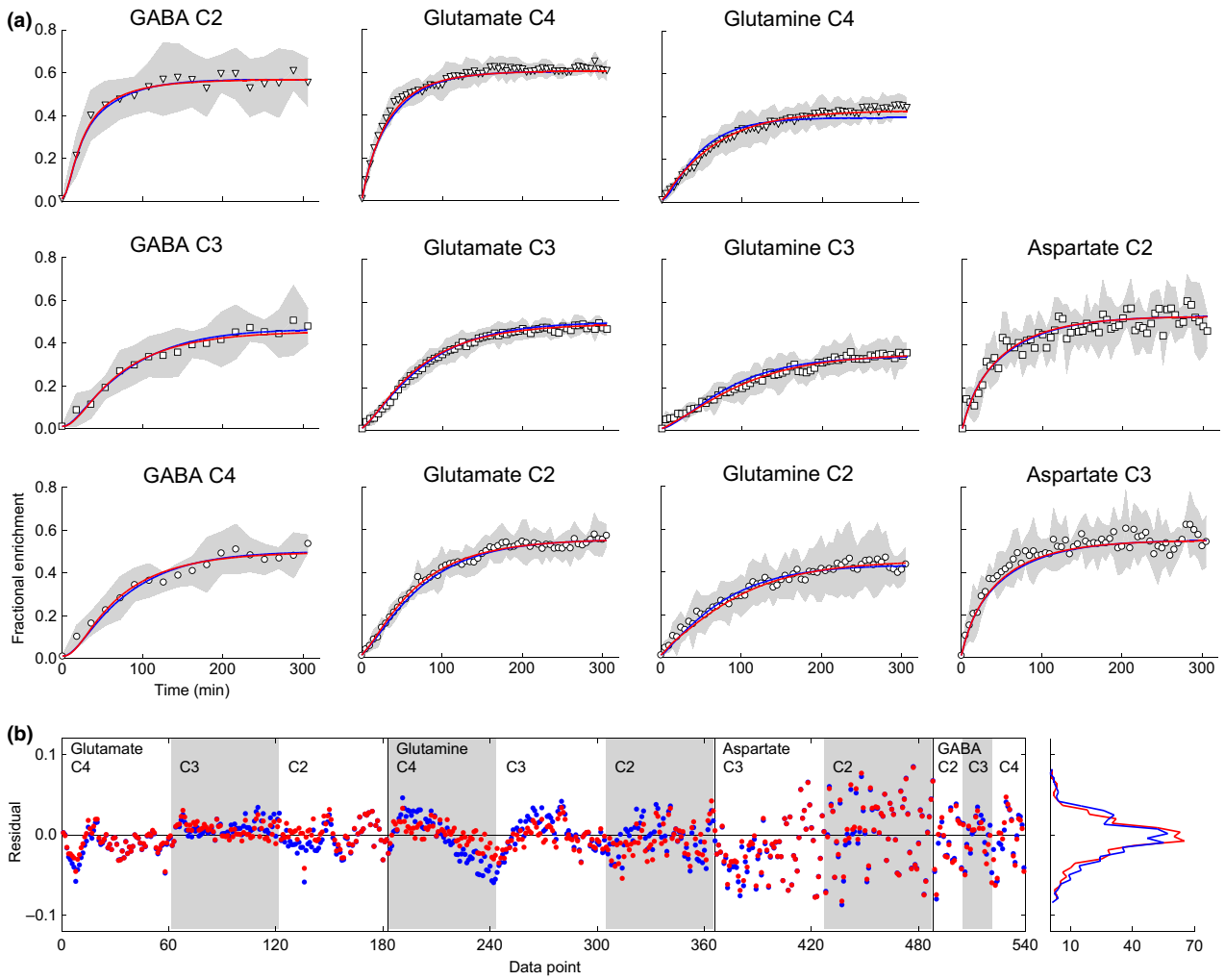

Fig. 4 Fractional enrichment in carbons of glutamate, glutamine, GABA and aspartate, and curves of the best fit of the three-compartment model (a). Data points are the mean of 8 rats, shaded area represents respective SD, blue and red lines depict the best fit to the data of the three-compartment model with one or two glial glutamine pools. Fit residuals of the models (b) with one (blue symbols) or two (red symbols) glial glutamine pools indicate fit improvement by addition of the glutamine pool with low ^{1}H NMR visibility. The lines on the right show the distribution of the residuals for each model.

aspects of metabolic compartmentation of GABA metabolism *in vivo*. GABA C4 but not C3 and C2 receives labelling from pyruvate through pyruvate carboxylation and thus it allowed to determine the contribution of glial metabolism to GABA synthesis, in addition to metabolic fluxes in GABAergic neurons (depicted in Fig. 1). In particular, we found that a considerable fraction of glucose was oxidized in the GABAergic compartment and connecting glial cells to fulfil the energetic requirements of GABAergic neurotransmission (13 ± 1%), and that glial glutamine accounts for an important fraction of GABA synthesis (48 ± 5%).

Detection of ^{13}C enrichment in GABA *in vivo* has been mostly accomplished using indirect detection of signals from ^{13}C-coupled protons. The first turnover curve of ^{13}C enriched GABA *in vivo* was reported by Pfeuffer *et al.* (1999), who measured GABA C3 in the rat brain during infusion of [1-^{13}C]glucose. Later, other GABA turnover curves were determined *in vivo* (e.g. Yang *et al.* 2005; van Eijsden *et al.* 2010). Although the indirect detection of ^{13}C-coupled protons has a high signal-to-noise ratio of protons, the low chemical shift dispersion, even at 14.1 T (Xin *et al.* 2010), results in substantial signal overlap. In contrast, the wide chemical shift dispersion of direct ^{13}C NMR spectra at high field allowed to quantify all three aliphatic GABA resonances. This study demonstrates the simultaneous quantification of the three aliphatic carbons of GABA with an average precision (CRLB) of 0.17 μmol/g (Fig. 3c) at a temporal resolution comparable to that of studies using ^{1}H-observed-^{13}C-edited spectroscopy methods (Pfeuffer *et al.* 1999; Yang *et al.* 2005; van Eijsden *et al.* 2010), a possibility that was not hitherto accessible at lower magnetic fields, especially for GABA C4, which partially overlaps

Table 2 Cerebral metabolic fluxes determined with the three-compartment model of [1,6-^{13}C]glucose metabolism. Estimated fluxes are shown in μmol/g/min with associated SD and *t*-value in parenthesis

		One glial glutamine pool R^2 = 0.972, f = 1680		With additional glutamine pool R^2 = 0.976, f = 1960	
Determined	V_{PDH}^{Glu} (= V_{TCA}^{Glu})	0.36 ± 0.01	(995)	0.33 ± 0.01	(931)
	V_{PDH}^{GABA}	0.024 ± 0.005	(174)	0.017 ± 0.005	(141)
	V_g	0.26 ± 0.02	(408)	0.29 ± 0.03	(409)
	V_{PC} (= V_{efflux})	0.076 ± 0.004	(704)	0.092 ± 0.005	(714)
	V_{dil}^g	1.1 ± 0.1	(189)	0.76 ± 0.07	(297)
	V_{NT}^{Glu}	0.16 ± 0.01	(381)	0.18 ± 0.01	(471)
	V_{NT}^{GABA} (= V_{shunt}^g)	0.044 ± 0.002	(504)	0.053 ± 0.003	(602)
	V_{GAD}^{GABA}	0.098 ± 0.003	(886)	0.11 ± 0.01	(970)
	V_x^{Glu}	0.41 ± 0.02	(568)	0.39 ± 0.02	(625)
	V_x^{GABA}	0.0067 ± 0.0038	(63.5)	0.0068 ± 0.0034	(77.5)
	V_x^g	0.010 ± 0.011	(28.4)	0.018 ± 0.018	(35.1)
	V_{ex}^g			0.060 ± 0.008	(284)
Calculated	$CMR_{glc(ox)}$	0.44 ± 0.02		0.47 ± 0.02	
	V_{out}	0.16 ± 0.03		0.11 ± 0.03	
	V_{TCA}^{GABA}	0.077 ± 0.007		0.070 ± 0.007	
	V_{TCA}^g	0.38 ± 0.02		0.44 ± 0.03	
	V_{shunt}^{GABA}	0.054 ± 0.004		0.053 ± 0.005	
	V_{GS}	0.28 ± 0.01		0.33 ± 0.01	
	V_{NT}^{total}	0.20 ± 0.01		0.24 ± 0.01	
	V_x^g + V_{PC} + V_{shunt}^g (OG→Glu)	0.13 ± 0.01		0.16 ± 0.02	
	V_x^{GABA} + V_{shunt}^{GABA} (OG→Glu)	0.060 ± 0.006		0.060 ± 0.006	

with the C3 of *N*-acetylaspartate (aspartyl moiety) (e.g. Choi and Gruetter 2003). The ability to quantify all GABA signals was ascribed to increased spectral resolution and high signal achieved at 14.1 T with surface coil signal detection, quantification by LCModel and use of [1,6-^{13}C]glucose infusion that leads to a nearly twofold increase in the fractional enrichment of observed metabolites, compared to the use of [1-^{13}C]glucose as substrate.

Cerebral metabolism of GABA and GABA-glutamine cycle

When comparing the fluxes obtained with the present three-compartment model (Fig. 1) to those obtained by fitting the previously published two-compartment model of brain energy metabolism (Duarte *et al.* 2011), we noted that most metabolic fluxes were not substantially different (Fig. 5a). Glucose oxidation was higher (0.47 ± 0.02 vs. 0.38 ± 0.02 μmol/g/min) and the net release of lactate (V_{out}) was 62 ± 11% lower than when using the two-compartment model (both with CMR_{glc} = 0.52 μmol/g/min). Thus, a substantial fraction of glucose utilization in the rat brain is involved in maintaining GABAergic function, rather than released as lactate. This indicates that the inclusion of a GABAergic compartment leads to a more complete account for total glucose metabolism.

A small but significant fraction of glucose was directly utilized in GABAergic neurons (7 ± 1% of total oxidation), as found by Patel *et al.* (2005) with quantification of ^{13}C GABA in brain extracts, suggesting that excitation plays an energetically dominant role. Anatomical and physiological data support the concept that inhibitory neurotransmission overall requires less energy compared to glutamatergic activity. Indeed, glutamatergic synapses outnumber GABAergic synapses by fivefold, with less than 30% of cortical neurons being inhibitory GABAergic interneurons (DeFelipe and Fariñas 1992; Sahara *et al.* 2012), and the energetic requirements of excitatory neurons have been suggested to be nearly three times those of inhibitory neurons (Howarth *et al.* 2012). Although it has been suggested that the recycling of GABA may not be coupled to glucose utilization in astrocytes, even though astrocytes respond to GABA by increasing intracellular sodium content (Chatton *et al.* 2003) according to the stechiometry of co-transport with two Na^+ and one Cl^- (Gadea and López-Colomé 2001), this does not preclude that activity of GABAergic nerve terminals *per se* does not involve energy consumption in neighbouring astrocytes. When providing simultaneously [U-^{13}C]glucose and [2-^{13}C]acetate to superfused hippocampal slices we previously found lower but significant contribution of acetate metabolized in glia to the multiplets of GABA, compared to those of glutamate, which further increases upon stimulation (Duarte *et al.* 2007).

It should be noted that the inclusion of GABAergic activity in the model lead to a substantial increment in the glial V_{TCA} to 47 ± 3% of total glucose oxidation (Fig. 5a), as part of it is required for GABA oxidation through the GABA shunt (12 ± 1% of V_{TCA}^g), which resulted in synthesis of glutamine

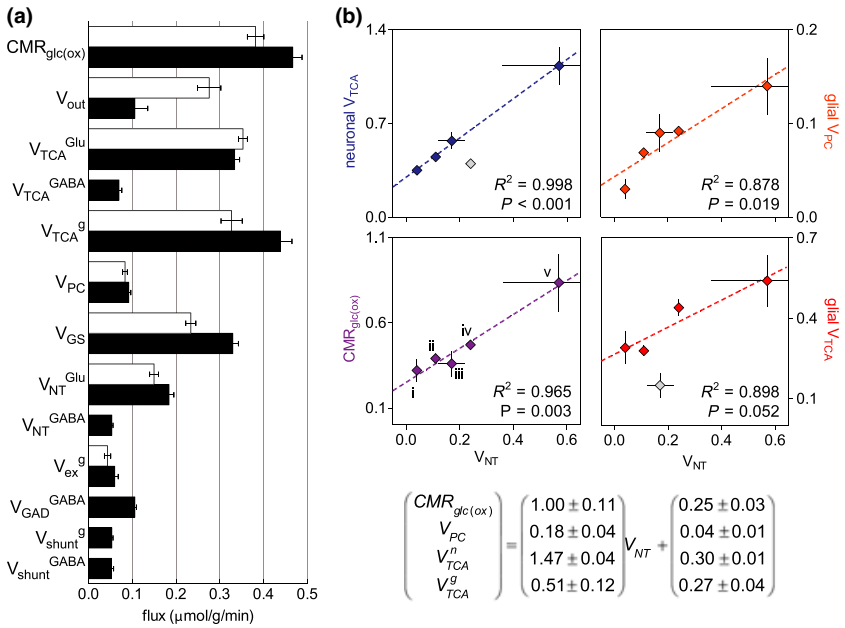

Fig. 5 Comparison of metabolic fluxes with those obtained from two-compartment models. (a) Shows fluxes obtained by fitting models of brain metabolism with three (filled bars) and two (open bars) compartments to the present data. The two-compartment model was adapted from Duarte *et al.* (2011) to include V_{ex}^{g}. (b) Shows the relation of estimated fluxes of total glucose oxidation, neuronal and glial TCA cycles and pyruvate carboxylation to glutamate/GABA-glutamine cycle, that is, total V_{NT}, across several studies using similar methodology in the rat or human brain: (i) rat brain under pentobarbital-induced isoelectricity (Choi *et al.* 2002), (ii) rat brain under light anaesthesia (Duarte *et al.* 2011), (iii) human cortex (Gruetter *et al.* 2001), (iv) current study, (v) awake rat brain (Oz *et al.* 2004). Metabolic fluxes are shown in μmol/g/min with associated SD. For linear regression, data sets (iv) and (iii) were excluded in V_{TCA}^{n} and V_{TCA}^{g}, respectively.

to be shuttled to GABAergic neurons for GABA production (16 ± 2% of V_{GS}). In this study, when accounting for this fraction of glial TCA cycle that is involved in supporting GABA recycling, the total glucose oxidation attributed to GABAergic function was 13 ± 1% of total $CMR_{glc(ox)}$.

Astrocytes lack the enzymatic machinery for GABA synthesis and, therefore, virtually all glial GABA originates from neuronal release (Schousboe and Waagepetersen 2003). In fact, we tested the presence of V_{GAD} in the glial compartment and this flux was consistently not significantly different from zero (not shown). Although not being able to synthesize GABA, astrocytes play an important role in GABA metabolism (reviewed in Schousboe *et al.* 1992; Choi and Shen 2012). In the present model, the flux through GAD was set to be equal to the sum of the glial and neuronal GABA shunts (thus respecting steady-state mass balance) that are associated with the respective GABA-T activities initiating GABA catabolism in mitochondria. Our results for V_{shunt}^{GABA} and V_{shunt}^{g} (Table 2) suggest that nearly half of GABA produced in GABAergic neurons is further oxidized in astrocytes through the glial GABA shunt and that half of GABA synthesis relies on glutamine provided by astrocytes, which is consistent with studies in cultured cortical neurons (Westergaard *et al.* 1995). This does not mean, however, that equal amounts of synaptically released GABA are taken up by astrocytes and neurons, while glutamate transporters in astrocytes largely exceed those in neurons, GABA transporters are mostly concentrated in membranes of GABAergic neurons (Conti *et al.* 2004), suggesting preferential uptake of glutamate by astrocytes and of GABA by neurons (e.g. Schousboe and Waagepetersen 2003, 2007; Bak *et al.* 2006). Thus, it may be suggested that a substantial amount of GABA released into the synapse must be taken up by same nerve terminal and directly re-incorporated into synaptic vesicles for subsequent release.

Glial metabolism supports neurotransmission

Since early studies of brain energy metabolism, it has been postulated that metabolic pathways leading to the production of energy are under direct control of cerebral activity (van den Berg *et al.* 1969). Aiming at elucidating how glucose metabolism is related to both glutamatergic and GABAergic synaptic transmission, we further compared the present results with previous reports in rodents and humans that considered all metabolic fluxes as independent parameters (Gruetter *et al.* 2001; Choi *et al.* 2002; Oz *et al.* 2004; Duarte *et al.* 2011). In general, the present results are in line with previous studies in either rodents or humans (Fig. 5b). Interestingly, in addition to glucose oxidation (Sibson *et al.* 1998), glial pyruvate carboxylation was related to the total neuron-glia neurotransmitter cycling (Fig. 5b). In fact, the activity-induced increase in glial anaplerosis through V_{PC} is

consistent with increased influx of bicarbonate into astrocytes upon neuronal release of K^+ (Chesler 1990; Brookes and Turner 1994) that may stimulate pyruvate carboxylation (Gamberino *et al.* 1997) along with modulation of glycolysis, glycogenolysis and lactate production (Choi *et al.* 2012). An intrinsic coupling between V_{PC}, V_{GS} and V_{efflux} was defined in the mathematical model, which finds support in the fact that increased brain activity leads to ammonia accumulation that likely requires detoxification through synthesis of glutamine that diffuses to the blood stream (suggested by Merle and Franconi 2012).

The total flux through pyruvate dehydrogenase in glia, depicted by $V_{TCA}{}^{g}$, also increased with V_{NT} in the rat brain. Because oxaloacetate produced from both pyruvate carboxylation and GABA oxidation require equivalent amount of acetyl-CoA for condensation, $V_{TCA}{}^{g}$ was defined as $V_g + V_{PC} + V_{shunt}{}^{g}$ (see Appendix), with V_g (that was 66 ± 8% of $V_{TCA}{}^{g}$) denoting the flux through glial pyruvate dehydrogenase corresponding to the complete oxidation of pyruvate (Gruetter *et al.* 2001). Interestingly, we did not observe a significant modification of V_g with V_{NT} (not shown), suggesting that pyruvate carboxylation and GABA oxidation are the main drive for the relation between glial V_{TCA} and V_{NT}, and that a large fraction of glial energy production is probably dedicated to non-signalling processes. In line with this, energy consumption for tasks unrelated to neurotransmission could account for up to ~ 50% of total energy expenditure in the whole rat brain (discussed in Howarth *et al.* 2012).

The relationship between the rates of glutamatergic neurotransmitter cycling and glucose oxidation in neurons is well established in the literature (e.g. Hyder *et al.* 2013). In agreement, oxidative metabolism in neurons was related with V_{NT} only for glutamatergic neurons, probably because GABA re-uptake is less energy demanding and GABAergic neurons receive substantial amount of glutamine synthesized *de novo* by astrocytes (discussed above). Increase of glial V_{TCA} with V_{NT} seemed to be species specific, being apparent that the data set from the human brain is not in line with those from rats.

Subcellular compartmentation of glial glutamine

In this study, we found that, when approaching isotopic steady-state, glutamine enrichment in C4 was similar to that in C2. This implies that glial dilution occurs and, therefore, V_{dil} was introduced to represent the utilization of glial-specific substrates that enter brain metabolism at the level of acetyl-CoA (see Duarte *et al.* 2011 and references therein). In addition, even when steady state of ^{13}C enrichment was reached for the mainly neuronal glutamate, GABA and aspartate, a significant and continuous increase in glutamine enrichment occurs (Fig. 4a) in the presence of a nearly constant total glutamine concentration, as measured *in vivo* using ^{1}H NMR spectroscopy under identical experimental conditions (Duarte *et al.* 2009; Duarte and Gruetter 2012). While pyruvate carboxylation could explain this effect in glutamine C3 and C2, the C4 only receives label from acetyl-CoA and thus should reach the steady-state enrichment together with the remaining amino acids. This continuous increase in brain glutamine enrichment upon ^{13}C-enriched glucose administration was also observed in previous studies using dynamic ^{13}C NMR spectroscopy *in vivo* in both rodents (Duarte *et al.* 2011) and humans (Shen *et al.* 1999).

Brain ^{13}C-enriched glutamine was found higher than total concentration of glutamine measured by ^{1}H NMR spectroscopy *in vivo*. This suggests that a fraction of brain glutamine is not visible in the ^{1}H NMR spectrum *in vivo*. In brain extracts, levels of glutamine relative to glutamate were similar to those measured *in vivo* (data not shown), suggesting that this putative glutamine pool with low NMR visibility (as suggested by Hancu and Port 2011) may be associated with macromolecules that precipitate upon perchloric acid extraction. The eventual existence of glutamine pools with different physical properties impelled us to test an alternative model with a fourth glutamine pool of the size of the non-visible glutamine, that is, difference between 5.3 ± 0.4 μmol/g and glutamine concentration measured by ^{1}H NMR spectroscopy. This pool was assumed to be in direct exchange with glial glutamine indicated by $V_{ex}{}^{g}$ (see Fig. 1).

The inclusion of a fourth glutamine pool in exchange with one of the other three (the glial pool) resulted in an approximation of the model curves to the measured data, namely glutamine carbons. This pool was found to be associated with a slow turnover and thus characterized by a nearly continuous increase in ^{13}C enrichment over the whole analysed time course. Astrocyte morphology is compatible with the existence of different functional domains and evidence from *in vitro* studies in cultured astrocytes using ^{13}C-labelled compounds may help unveil the existence of multiple glial glutamine pools: in addition to mitochondrial heterogeneity and glutamine synthesis from multiple TCA cycles (Sonnewald *et al.* 1998; Waagepetersen *et al.* 2006), intracellular and released glutamine displayed distinct labelling patters from metabolism of ^{13}C-enriched glucose and lactate (Waagepetersen *et al.* 2001). Together with our results, these observations support the existence of a glial glutamine pool with slow turnover that is not released to neurons but could be used for protein synthesis or eventually metabolized for energy production (discussed in McKenna 2007). In alternative, it is possible that metabolic heterogeneity occurs within the astrocytic syncytium or that multiple glial compartments are present in the volume of interest encompassing distinct brain areas. This scenario is however difficult to model because of the large number of parameters to be estimated from the observed ^{13}C enrichment curves.

Mitochondrial membrane transport

Labelling of brain glutamate from ^{13}C-enriched oxidative substrates requires transfer of the label from the mitochondrial TCA cycle intermediate 2-oxoglutarate to cytosolic glutamate, mainly via the 2-oxoglutarate-malate and glutamate-aspartate carriers in the mitochondrial membrane, which also sustains the transfer of reducing equivalents from cytosol to mitochondria. In the compartments where the GABA shunt occurs, that is, glia and GABAergic neurons, a substantial part of 2-oxoglutarate transamination to glutamate occurred with GABA (V_{shunt}), yielding SSA that is further metabolized by the TCA cycle. Mitochondrial transport of ^{13}C label in glia, that is, $V_X^g + V_{PC} + V_{shunt}^g$ that includes GABA transamination and net glutamate synthesis, was much lower than the neuronal counterpart, which is in agreement with the finding that carriers exchanging aspartate and glutamate in the malate-aspartate shuttle are predominantly expressed in neurons rather than astrocytes (Ramos *et al.* 2003; Berkich *et al.* 2007; Pardo *et al.* 2011). In contrast, Li *et al.* recently found comparable amounts of Aralar protein, the main mitochondrial carrier for aspartate/glutamate in the brain, in freshly isolated neurons and astrocytes (Li *et al.* 2012), suggesting that the transference of reducing equivalents across the mitochondrial membrane is not a limiting step for adaptation to altered metabolic or energetic demand in astrocytes.

Although the rate of label transfer from 2-oxoglutarate to glutamate is frequently thought to occur at a more rapid rate than that of TCA cycle intermediate oxidation (e.g. Mason *et al.* 1995; Sibson *et al.* 1998; Yang *et al.* 2009), metabolic modelling of ^{13}C NMR data from humans (Gruetter *et al.* 2001) and rats (Choi *et al.* 2002; Oz *et al.* 2004; Duarte *et al.* 2011) with independent flux estimation found mitochondrial exchange fluxes on the order of the TCA cycle rate, as observed in this study. The present data were only consistent with mitochondrial exchange fluxes in the same order of the respective TCA cycle rates and the constraint of V_X to be 10 times greater than V_{TCA} in each compartment lead to large fit residuals (not shown). This conclusion is further strengthened by the finding that under near physiological conditions the rate of 2-oxoglutarate synthesis in brain mitochondria was similar to that of α-ketoglutarate/glutamate efflux (Berkich *et al.* 2005). Furthermore, 2-oxoglutarate but not glutamate was detected in the rat brain by ^{13}C NMR spectroscopy upon infusion of hyperpolarized acetate (Mishkovsky *et al.* 2012).

Conclusion

We conclude that GABAergic neurons consume a substantial fraction of glucose and that glutamine of glial origin is an important precursor for GABA synthesis in the rat brain *in vivo*. This is in line with the metabolic cooperation between astrocytes and neurons for maintenance of not only excitatory but also inhibitory neurotransmission. Furthermore, subcellular metabolic compartmentation, namely in astrocytes, can improve description of the experimental data with mathematical models of brain metabolism.

Acknowledgements

This study was supported by Swiss National Science Foundation (grant 131087) and by Centre d'Imagerie BioMédicale (CIBM) of the UNIL, UNIGE, HUG, CHUV, EPFL and the Leenaards and Jeantet Foundations. The authors are grateful to Patricia M. Nunes (Radboud University Nijmegen Medical Centre, Nijmegen) and Dr. Bernard Lanz (LIFMET) for fruitful discussions and to Jessica A.M. Bastiaansen (LIFMET) for help with preparation of figures. The authors declare no conflicts of interest.

Supporting information

Additional supporting information may be found in the online version of this article at the publisher's web-site.

Appendix S1. Three-compartment model of [1,6-^{13}C]glucose metabolism in the brain.

References

Bak L. K., Schousboe A. and Waagepetersen H. S. (2006) The glutamate/GABA-glutamine cycle: aspects of transport, neurotransmitter homeostasis and ammonia transfer. *J. Neurochem.* **98**, 641–653.

van den Berg C. J., Krzalić L., Mela P. and Waelsch H. (1969) Compartmentation of glutamate metabolism in brain. Evidence for the existence of two different tricarboxylic acid cycles in brain. *Biochem. J.* **113**, 281–290.

Berkich D. A., Xu Y., LaNoue K. F., Gruetter R. and Hutson S. M. (2005) Evaluation of brain mitochondrial glutamate and alpha-ketoglutarate transport under physiologic conditions. *J. Neurosci. Res.* **79**, 106–113.

Berkich D. A., Ola M. S., Cole J., Sweatt A. J., Hutson S. M. and LaNoue K. F. (2007) Mitochondrial transport proteins of the brain. *J. Neurosci. Res.* **85**, 3367–3377.

Brookes N. and Turner R. J. (1994) K^+-induced alkalinization in mouse cerebral astrocytes mediated by reversal of electrogenic Na^+-HCO_3^- cotransport. *Am. J. Physiol.* **267**, C1633–C1640.

Calvetti D. and Somersalo E. (2012) Ménage à trois: the role of neurotransmitters in the energy metabolism of astrocytes, glutamatergic, and GABAergic neurons. *J. Cereb. Blood Flow Metab.* **32**, 1472–1483.

Chatton J. Y., Pellerin L. and Magistretti P. J. (2003) GABA uptake into astrocytes is not associated with significant metabolic cost: implications for brain imaging of inhibitory transmission. *Proc. Natl Acad. Sci. USA* **100**, 12456–12461.

Chesler M. (1990) The regulation and modulation of pH in the nervous system. *Prog. Neurobiol.* **34**, 401–427.

Choi I. Y. and Gruetter R. (2003) *In vivo* ^{13}C NMR assessment of brain glycogen concentration and turnover in the awake rat. *Neurochem. Int.* **43**, 317–322.

Choi I.-Y. and Shen J. (2012) *In vivo* GABA metabolism, in *Neural Metabolism In Vivo* (Choi I.-Y. and Gruetter R., eds), pp. 1095–1116. Springer, New York.

Choi I. Y., Lei H. and Gruetter R. (2002) Effect of deep pentobarbital anesthesia on neurotransmitter metabolism *in vivo*: on the correlation of total glucose consumption with glutamatergic action. *J. Cereb. Blood Flow Metab.* **22**, 1343–1351.

Choi H. B., Gordon G. R., Zhou N. *et al.* (2012) Metabolic communication between astrocytes and neurons via bicarbonate-responsive soluble adenylyl cyclase. *Neuron* **75**, 1094–1104.

Conti F., Minelli A. and Melone M. (2004) GABA transporters in the mammalian cerebral cortex: localization, development and pathological implications. *Brain Res. Brain Res. Rev.* **45**, 196–212.

DeFelipe J. and Fariñas I. (1992) The pyramidal neuron of the cerebral cortex: morphological and chemical characteristics of the synaptic inputs. *Prog. Neurobiol.* **39**, 563–607.

Duarte J. M. N. and Gruetter R. (2012) Characterization of cerebral glucose dynamics *in vivo* with a four-state conformational model of transport at the blood-brain-barrier. *J. Neurochem.* **121**, 396–406.

Duarte J. M. N., Cunha R. A. and Carvalho R. A. (2007) Different metabolism of glutamatergic and GABAergic compartments in superfused hippocampal slices characterized by nuclear magnetic resonance spectroscopy. *Neuroscience* **144**, 1305–1313.

Duarte J. M. N., Carvalho R. A., Cunha R. A. and Gruetter R. (2009) Caffeine consumption attenuates neurochemical modifications in the hippocampus of streptozotocin-induced diabetic rats. *J. Neurochem.* **111**, 368–379.

Duarte J. M. N., Lanz B. and Gruetter R. (2011) Compartmentalized cerebral metabolism of [1,6-^{13}C]glucose Determined by *in vivo* ^{13}C NMR spectroscopy at 14.1 T. *Front. Neuroenergetics* **3**, 3.

van Eijsden P., Behar K. L., Mason G. F., Braun K. P. and de Graaf R. A. (2010) *In vivo* neurochemical profiling of rat brain by ^{1}H-[^{13}C] NMR spectroscopy: cerebral energetics and glutamatergic/GABAergic neurotransmission. *J. Neurochem.* **112**, 24–33.

Gadea A. and López-Colomé A. M. (2001) Glial transporters for glutamate, glycine, and GABA: II. GABA transporters. *J. Neurosci. Res.* **63**, 461–468.

Gamberino W. C., Berkich D. A., Lynch C. J., Xu B. and LaNoue K. F. (1997) Role of pyruvate carboxylase in facilitation of synthesis of glutamate and glutamine in cultured astrocytes. *J. Neurochem.* **69**, 2312–2325.

Gruetter R. (1993) Automatic, localized *in vivo* adjustment of all first- and second-order shim coils. *Magn. Reson. Med.* **29**, 804–811.

Gruetter R. (2002) *In vivo* ^{13}C NMR studies of compartmentalized cerebral carbohydrate metabolism. *Neurochem. Int.* **41**, 143–154.

Gruetter R. and Tkác I. (2000) Field mapping without reference scan using asymmetric echo-planar techniques. *Magn. Reson. Med.* **43**, 319–323.

Gruetter R., Novotny E. J., Boulware S. D., Mason G. F., Rothman D. L., Shulman G. I., Prichard J. W. and Shulman R. G. (1994) Localized ^{13}C NMR spectroscopy in the human brain of amino acid labeling from D-[1-^{13}C]glucose. *J. Neurochem.* **63**, 1377–1385.

Gruetter R., Seaquist E. R. and Ugurbil K. (2001) A mathematical model of compartmentalized neurotransmitter metabolism in the human brain. *Am. J. Physiol. Endocrinol. Metab.* **281**, E100–E112.

Hancu I. and Port J. (2011) The case of the missing glutamine. *NMR Biomed.* **24**, 529–535.

Henry P. G., Tkác I. and Gruetter R. (2003a) ^{1}H-localized broadband ^{13}C NMR spectroscopy of the rat brain *in vivo* at 9.4 T. *Magn. Reson. Med.* **50**, 684–692.

Henry P. G., Oz G., Provencher S. and Gruetter R. (2003b) Toward dynamic isotopomer analysis in the rat brain *in vivo*: automatic quantitation of ^{13}C NMR spectra using LCModel. *NMR Biomed.* **16**, 400–412.

Howarth C., Gleeson P. and Attwell D. (2012) Updated energy budgets for neural computation in the neocortex and cerebellum. *J. Cereb. Blood Flow Metab.* **32**, 1222–1232.

Hyder F., Fulbright R. K., Shulman R. G. and Rothman D. L. (2013) Glutamatergic function in the resting awake human brain is supported by uniformly high oxidative energy. *J. Cereb. Blood Flow Metab.* **33**, 339–347.

Li B., Hertz L. and Peng L. (2012) Aralar mRNA and protein levels in neurons and astrocytes freshly isolated from young and adult mouse brain and in maturing cultured astrocytes. *Neurochem. Int.* **61**, 1325–1332.

Malloy C. R., Sherry A. D. and Jeffrey F. M. (1987) Carbon flux through citric acid cycle pathways in perfused heart by 13C NMR spectroscopy. *FEBS Lett.* **212**, 58–62.

Mason G. F., Gruetter R., Rothman D. L., Behar K. L., Shulman R. G. and Novotny E. J. (1995) Simultaneous determination of the rates of the TCA cycle, glucose utilization, alpha-ketoglutarate/glutamate exchange, and glutamine synthesis in human brain by NMR. *J. Cereb. Blood Flow Metab.* **15**, 12–25.

McKenna M. C. (2007) The glutamate-glutamine cycle is not stoichiometric: fates of glutamate in brain. *J. Neurosci. Res.* **85**, 3347–3358.

Merle M. and Franconi J.-M. (2012) Brain metabolic compartmentalization, metabolism modeling, and cerebral activity-metabolism relationship, in *Neural Metabolism In Vivo* (Choi I.-Y. and Gruetter R., eds), pp. 947–992. Springer, New York.

Mishkovsky M., Comment A. and Gruetter R. (2012) *In vivo* detection of brain Krebs cycle intermediate by hyperpolarized magnetic resonance. *J. Cereb. Blood Flow Metab.* **32**, 2108–2113.

Mlynárik V., Gambarota G., Frenkel H. and Gruetter R. (2006) Localized short-echo-time proton MR spectroscopy with full signal-intensity acquisition. *Magn. Reson. Med.* **56**, 965–970.

Oz G., Berkich D. A., Henry P. G., Xu Y., LaNoue K., Hutson S. M. and Gruetter R. (2004) Neuroglial metabolism in the awake rat brain: CO_2 fixation increases with brain activity. *J. Neurosci.* **24**, 11273–11279.

Pardo B., Rodrigues T. B., Contreras L., Garzón M., Llorente-Folch I., Kobayashi K., Saheki T., Cerdan S. and Satrústegui J. (2011) Brain glutamine synthesis requires neuronal-born aspartate as amino donor for glial glutamate formation. *J. Cereb. Blood Flow Metab.* **31**, 90–101.

Patel A. B., de Graaf R. A., Mason G. F., Rothman D. L., Shulman R. G. and Behar K. L. (2005) The contribution of GABA to glutamate/glutamine cycling and energy metabolism in the rat cortex *in vivo*. *Proc. Natl Acad. Sci. USA* **102**, 5588–5593.

Pfeuffer J., Tkác I., Choi I. Y., Merkle H., Ugurbil K., Garwood M. and Gruetter R. (1999) Localized *in vivo* ^{1}H NMR detection of neurotransmitter labeling in rat brain during infusion of [1-^{13}C] D-glucose. *Magn. Reson. Med.* **41**, 1077–1083.

Ramos M., del Arco A., Pardo B. *et al.* (2003) Developmental changes in the Ca^{2+}-regulated mitochondrial aspartate-glutamate carrier aralar1 in brain and prominent expression in the spinal cord. *Dev. Brain Res.* **143**, 33–46.

Sahara S., Yanagawa Y., O'Leary D. D. and Stevens C. F. (2012) The fraction of cortical GABAergic neurons is constant from near the start of cortical neurogenesis to adulthood. *J. Neurosci.* **32**, 4755–4761.

Schousboe A. and Waagepetersen H. S. (2003) Role of astrocytes in homeostasis of glutamate and GABA during physiological and pathophysiological conditions. *Adv. Mol. Cell Biol.* **31**, 461–474.

Schousboe A. and Waagepetersen H. S. (2007) GABA: homeostatic and pharmacological aspects. *Prog. Brain Res.* **160**, 9–19.

Schousboe A., Westergaard N., Sonnewald U., Petersen S. B., Yu A. C. and Hertz L. (1992) Regulatory role of astrocytes for neuronal biosynthesis and homeostasis of glutamate and GABA. *Prog. Brain Res.* **94**, 199–211.

Shen J., Petersen K. F., Behar K. L., Brown P., Nixon T. W., Mason G. F., Petroff O. A., Shulman G. I., Shulman R. G. and Rothman D. L.

(1999) Determination of the rate of the glutamate/glutamine cycle in the human brain by *in vivo* ^{13}C NMR. *Proc. Natl Acad. Sci. USA* **96**, 8235–8240.

Shestov A. A., Valette J., Uğurbil K. and Henry P. G. (2007) On the reliability of ^{13}C metabolic modeling with two-compartment neuronal-glial models. *J. Neurosci. Res.* **85**, 3294–3303.

Sibson N. R., Dhankhar A., Mason G. F., Rothman D. L., Behar K. L. and Shulman R. G. (1998) Stoichiometric coupling of brain glucose metabolism and glutamatergic neuronal activity. *Proc. Natl Acad. Sci. USA* **95**, 316–321.

Sonnewald U., Hertz L. and Schousboe A. (1998) Mitochondrial heterogeneity in the brain at the cellular level. *J. Cereb. Blood Flow Metab.* **18**, 231–237.

Tkác I., Rao R., Georgieff M. K. and Gruetter R. (2003) Developmental and regional changes in the neurochemical profile of the rat brain determined by *in vivo* ^{1}H NMR spectroscopy. *Magn. Reson. Med.* **50**, 24–32.

Waagepetersen H. S., Sonnewald U. and Schousboe A. (1999) The GABA paradox: multiple roles as metabolite, neurotransmitter, and neurodifferentiative agent. *J. Neurochem.* **73**, 1335–1342.

Waagepetersen H. S., Sonnewald U., Larsson O. M. and Schousboe A. (2001) Multiple compartments with different metabolic characteristics are involved in biosynthesis of intracellular and released glutamine and citrate in astrocytes. *Glia* **35**, 246–252.

Waagepetersen H. S., Hansen G. H., Fenger K., Lindsay J. G., Gibson G. and Schousboe A. (2006) Cellular mitochondrial heterogeneity in cultured astrocytes as demonstrated by immunogold labeling of alpha-ketoglutarate dehydrogenase. *Glia* **53**, 225–231.

Westergaard N., Sonnewald U., Petersen S. B. and Schousboe A. (1995) Glutamate and glutamine metabolism in cultured GABAergic neurons studied by ^{13}C NMR spectroscopy may indicate compartmentation and mitochondrial heterogeneity. *Neurosci. Lett.* **185**, 24–28.

Xin L., Mlynárik V., Lanz B., Frenkel H. and Gruetter R. (2010) ^{1}H-[^{13}C] NMR spectroscopy of the rat brain during infusion of [2-^{13}C] acetate at 14.1 T. *Magn. Reson. Med.* **64**, 334–340.

Yang J., Li C. Q. and Shen J. (2005) *In vivo* detection of cortical GABA turnover from intravenously infused [1-^{13}C]D-glucose. *Magn. Reson. Med.* **53**, 1258–1267.

Yang J., Xu S. and Shen J. (2009) Fast isotopic exchange between mitochondria and cytosol in brain revealed by relayed ^{13}C magnetization transfer spectroscopy. *J. Cereb. Blood Flow Metab.* **29**, 661–669.